Vol. 32 No. 136 *Journal of the Radio Research Laboratory* *July 1985*
Printed in Tokyo, Japan *pp. 99–121*

AN ANALYSIS OF THE BASELINE DETERMINATION BETWEEN JAPAN AND U.S. STATIONS BY USING THE VLBI DATA IN THE SYSTEM-LEVEL EXPERIMENTS

By
Yukio TAKAHASHI, Kunimasa KOIKE, Taizoh YOSHINO,
and Seiji MANABE*

(Received on March 22, 1985)

ABSTRACT

The system-level experiments on the Japan-U.S. joint VLBI (Very Long Baseline Interferometry) project were conducted in January and February, 1984. These experiments were carried out to ensure the overall performance of K-3 VLBI system and to determine precisely the baseline-length between Kashima Station and Mojave Base Station. Over five hundred observations were successfully performed in the two experiments. The correlation processing was made by both K-3 processor at Kashima and Mark-III processor at Haystack. The two baseline-lengths between Kashima and Mojave obtained in the two experiments show excellent repeatability. The precision of the baseline-length is adjusted to be higher than 0.02 m in root mean square.

According to these results, it is confirmed that K-3 system has the expected performance, and that the baseline-length between Kashima and Mojave is 8091824.11 m with a precision of 0.02 m.

1. Introduction

Radio Research Laboratory (RRL) has developed a system compatible with the U.S. Mark-III VLBI system which we call K-3 system for the Japan-U.S. joint experiments. RRL developed a part of analysis software of K-3 system with the cooperation of International Latitude Observatory of Mizusawa (ILOM).

Just after the K-3 system development, the Japan-U.S. system-level experiments were carried out twice, that is, between Kashima and Mojave on 23–24 January 1984, and between any two of Kashima, Mojave and Hat Creek on 24–25 February 1984. Hat Creek participated only in the February experiment. Each experiment covered 24 hours.

Fig. 1 shows the location of the three stations which participated in these experiments. The baseline between Kashima and Mojave takes a direction of almost east-west, and its length is about 8100 km. The baseline between Kashima and Hat Creek takes almost the same direction and length. The baseline between Mojave and Hat Creek takes a direction of almost northwest-southeast and its length is about 730 km.

Each observation time was 380 seconds and receiving frequencies were from 8211 MHz to 8571 MHz in X-band and from 2218 MHz to 2303 MHz in S-band. Observations were conducted 152 times in January and 136 times in February.

* International Latitude Observatory of Mizusawa

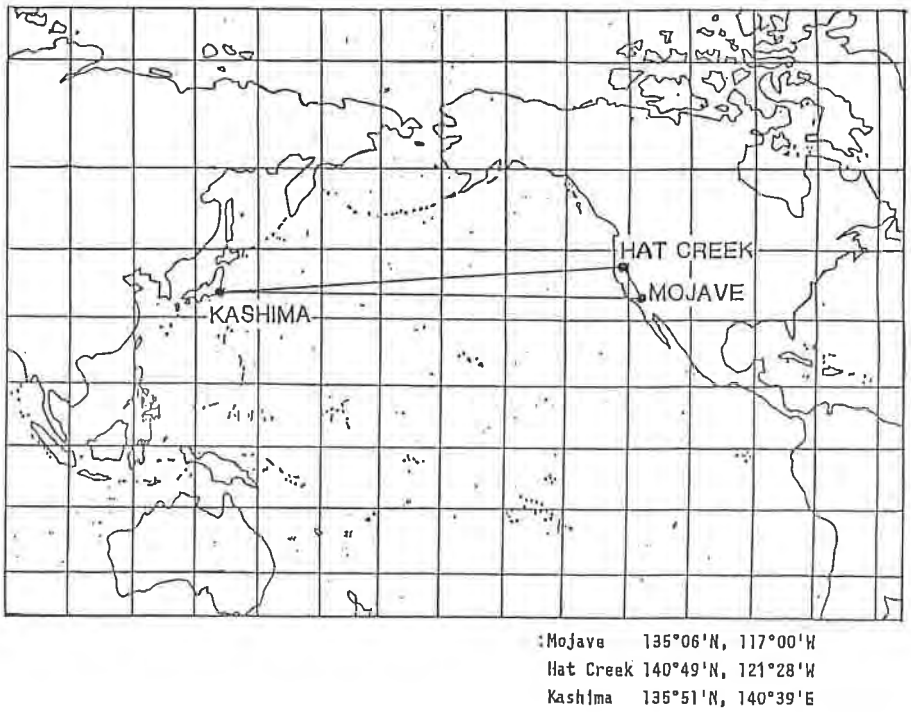

Fig. 1 Location of stations participating in US-Japan VLBI experiments.

K-3 system adopts IEEE-488 Bus for the communication between the computer and each part of all the hardware. The system is operated by the "KAOS" software, which is compatible with the Field System of Mark-III.

2. Correlation Processing

Fig. 2 shows the block diagram of the processing and data analysis. A large quantity of observed data is processed by K-3 correlation processing system. It consists of one correlation processor, two data recorders, two computer systems, and correlation processing software "KROSS" which corresponds to "COREL" of Mark-III. The processor has 4 correlation crates, each of which can process 8 pairs of data streams. "KROSS" has two main functions. One is the hardware control for data processing, and the other is the parameter set for the processing. In the former case, the main operation is the synchronization of the two data recorders. In the latter case, "KROSS" calculates a priori delays, delay-rates and delay accelerations, then transforms them into the format acceptable in the correlator. Correlation data per 1 pp (parameter period) make one file in HP1000/45F through IEEE-488 Bus.

Bandwidth synthesis is made by "KOMB" which corresponds to "FRNGE" of Mark-III by using correlation data files. The delays and delay-rates generated by "KOMB" are put into data base.

The following discussions are concerned with the comparison of the processing results

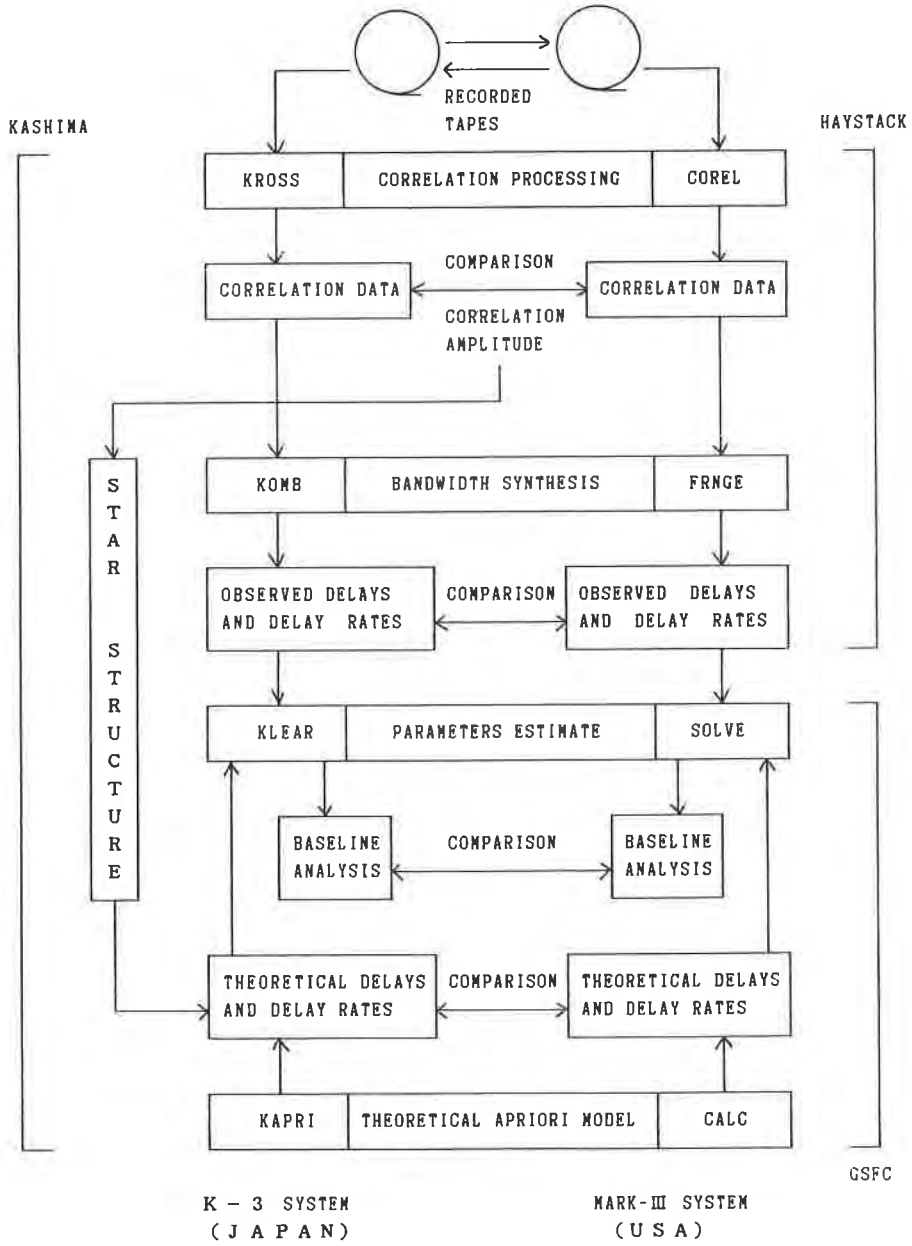

Fig. 2 Correlation processing and baseline analysis.

obtained by Kashima and Haystack. Since we neglected the delay acceleration by the atmosphere, some of our correlation results had low quality in the following three points. We already improved the a priori values of delay accelerations by atmosphere, so our correlation results for the coming experiments are now as good as those obtained by Mark-III.

(1) Fringe Amplitude

Fringe amplitudes of observations at low elevation are often smaller than those of Mark-III by about 10% in the average.

(2) Closure Delay and Delay-rate

Standard deviations of X band closure delays and delay-rates are 0.099 nsec and 0.099 psec/sec in our correlation results. In this calculation, data more than 0.5 nsec for delay and 0.5 psec/sec for delay-rate are excluded. In Mark-III they are 0.074 nsec in delay and 0.021 psec/sec in delay-rate respectively.

(3) Observed Delays and Delay-rates

We compare the differences in delays and delay-rates between K-3 and Mark-III. The standard diviations of such differences are 0.052 nsec for delays and 0.12 psec/sec for delay-rates in these experiments. It seems that the delay-rates obtained by K-3 are scattered more than those obtained by Mark-III. This is the same as the closure test mentioned above.

Data integration time is shorter than the duration of observation because of the data loss in synchronizing the recorders. In K-3 processing, it requires about 60 seconds to synchronize both recorders. The average integration time in K-3 is 290 seconds, which is a little worse than the one in Haystack because of our sophisticated software design and the slow computer access. This is not so serious a problem now, but we have been shortening the loss time.

3. Geophysical and Astronomical Models

Prior to the adjustment of geodetic, geophysical and astronomical parameters by VLBI data, it is necessary to predict VLBI variables as accurately as possible because inaccurate values of unadjusted parameters cause systematic biases in adjusted parameters. "KAPRI" is a program to compute theoretical (or more commonly, a priori) values. In addition, it computes contributions of individual physical effects to the observables as well as partial derivatives of the observables with respect to the adjustment of parameters which model the contributing physical effects.

In order to compute the VLBI observables theoretically we adopt, in "KAPRI", geophysical and astronomical models which are currently considered to be most accurate. In particular, attention is paid to the consistent use of dynamical models of the Earth and of relativistic effects. We also adopt the internationally approved system of constants, that is, the MERIT (Monitor Earth Rotation and Intercompare the Techniques of observation and analysis) standards (Melbourne et al. 1983)[1]. Moreover, in some points, we use more elaborate models.

Two terrestrial coordinate systems are used in "KAPRI". One is the VLBI coordinate system to which the coordinates of observation sites are referred. The other is defined by the

Conventional International Origin (CIO) and the Bureau International de l'Heure (BIH) zero meridian. This coordinate system is used when the Earth orientation parameters are concerned. The VLBI coordinate system as well as its relationship with other coordinate systems will be described in detail in the next section.

Geophysical and astronomical effects as well as geometric effects which are necessary to compute theoretical delay and delay-rate are classified as follows:

(1) Variations of an instantaneous position of a reference point of an antenna referred to a terrestrial reference system (antenna axis offset, solid Earth tide and ocean tidal loading),
(2) Rotation of a terrestrial reference system relative to a celestial reference system at a reference epoch, namely, J2000.0 (polar motion, diurnal rotation, nutation and precession),
(3) Relativistic effects (transformation of the time system from International Atomic Time (TAI) to Barycentric Dynamical Time (TDB) and vice versa, Lorentz space contraction),
(4) Variations of apparent star places expressed by a celestial reference system at a reference epoch (gravitational bending of radio wave, parallax and proper motion),
(5) Effects of propagation media (solar corona, ionosphere, dry and wet components of atmosphere).

Of the effects mentioned above, we neglect parallax and proper motion. In fact, QSO are considered to be so distant that their parallaxes and proper motions are quite small, if we neglect the variation of brightness distribution of radio sources. In the following sections we briefly describe the individual models used in "KAPRI" in the above order.

3.1 Antenna Axis Offset

A fixed reference point of an antenna is the intersection of the fixed axis with the plane containing the moving axis and perpendicular to it. If the antenna axes do not intersect, there is a distance between the moving axis and the reference point. This distance is called "Antenna Axis Offset".

If the antenna axis offset is not zero, the difference in time along the radio wave path to the feed and the radio wave path to the reference point changes as elevation and azimuth change. "KAPRI" includes the correction of the antenna axis offset for the delay and delay-rate.

3.2 Earth Tide

Displacement of an observation site due to the solid Earth tides is computed on the basis of the harmonic expansion of the lunisolar tidal potential by Cartwright and Tayler (1971)[2] and by Cartwright and Edden (1973)[3], and on Love and Shida numbers by Wahr (1981)[4]. All of the 484 frequency components of the expanded tidal potential are included. Since Wahr gave Love and Shida numbers for only major components in the diurnal band, we compute them for the rest of the diurnal constituents, by using his interpolation formulae. We use the lunisolar arguments given in the MERIT standards, which are also used in the computation of nutation, rather than the original arguments given in the paper by Cartwright and Tayler (1971)[2].

The computing scheme in the MERIT standards is much simpler than ours. In the MERIT standards the resonance effect of the Earth's fluid core is taken into account only

for several waves. Although our procedure requires much more computer time than the MERIT standards, we dare to take full account of the theories, because it is the clearest way to keep consistency between the treatments of the Earth tides and of the nutation which is another response of the Earth to the lunisolar gravitational attraction.

3.3 Ocean Tidal Loading

Effects of the tidal loading of ocean on site displacements are not negligibly small for sites near the ocean. In fact, Kashima is located only 3 km away from the coast of the Pacific Ocean. The site displacement due to the ocean loading is computed on the bases of Schwiderski's (1978)[5] ocean tidal models and of Farrell's (1972)[6] load Love numbers. Sato and Hanada (1984)[7] developed a more advanced method than Goad's (1980)[8] whose results are adopted in the MERIT standards. Using tide gauge observations at Kashima Port near Kashima Station, RRL, they computed the effect of the ocean loading at Kashima for nine frequencies. The results are shown in Table 1. It is likely that total upward displacement at Kashima exceeds 0.03 m.

Table 1 Displacement of Kashima by Ocean Tidal Loading (From Sato and Hanada)[7]

TIDAL COMPONENT	RADIAL DISPLACEMENT		N–S DISPLACEMENT		E–W DISPLACEMENT	
	AMP. (cm)	PHASE (DEG)	AMP. (cm)	PHASE (DEG)	AMP. (cm)	PHASE (DEG)
M2	0.90126	333.31	0.18259	205.57	0.30591	186.35
S2	0.46641	355.68	0.06732	220.33	0.14703	226.20
K1	1.1308	2.20	0.16833	53.89	0.23917	242.11
O1	0.88148	342.93	0.12134	34.50	0.18962	221.13
N2	0.14113	346.49	0.03672	191.75	0.03939	178.39
P1	0.35976	2.09	0.05086	56.79	0.07558	242.12
K2	0.12831	0.77	0.02176	226.07	0.03928	228.20
Q1	0.18808	337.10	0.02226	20.66	0.03912	218.93
Mf	0.01472	164.61	0.00456	41.42	0.00367	135.85

The Earth model used by Farrell is Gutenberg-Bullen's one (see Alterman et al. 1961[9]). Therefore, the ocean tidal effects are not based on the same Earth model as the nutation and solid Earth tide are. However, the difference between the Earth models is quite small, since the ocean tidal effects themselves are small.

3.4 Wobble

There are three sources which provide coordinates of the pole usable as a priori values in "KAPRI". They are BIH Circular D, International Polar Motion Service (IPMS) daily values and International Radio Interferometric Surveying (IRIS) data values. Instantaneous values of the coordinates of the pole are computed by interpolating 5-day values for the BIH and daily values for the IPMS.

The origin of the IPMS values was adjusted to BIH's throughout the year of 1980.

Nevertheless, there are discrepancies between them, especially in early 1984 when the first Japan-U.S. experiments were conducted. The discrepancy in this period amounted to 0.024 second of arc and brought about significant changes in final results of the baseline adjustment which are described later.

3.5 UT1

BIH Circular D and IPMS daily optimum values are used as a priori values. Instantaneous values of UT1-UTC are computed in the same way as the wobble.

Major difference of our UT1 model from others such as the MERIT standards is that our UT1 model has the option to account for the variation of UT1 due to the zonal tides with periods longer than a month (Yoder et al. 1981)[10]. Necessity of these longer periodic components has been demonstrated by Naito and Yokoyama (1984)[11]. They showed that correcting for the semi-annual component significantly reduces discrepancies between length-of day's (l.o.d.'s) derived from the IPMS optical astrometry observations and from variations of atmospheric angular momentum.

3.6 Nutation

The IAU 1980 nutation theory (Wahr 1981[12]; Kinoshita 1977[13]), which is also included in the MERIT standards, is adopted. It is based upon 1066A Earth model of Gilbert and Dziewonski (1975)[14] which includes effects of a solid inner core, liquid outer core and mantle with distributed elasticity. However, Wahr's theory does not take account of effects of viscosity of the liquid outer core or those of the ocean. It is quite interesting to observationally determine dissipative processes inside and on the Earth, such as the core viscosity as well as inelasticity of the mantle. VLBI may be one of the most promising methods to determine them by detecting the phase lags of the nutation. Therefore, we compute partial derivatives of the delay and delay-rate with respect to some major components of the nutation.

3.7 Precession

The precession parameters used rigorously follow the MERIT standards (Lieske et al. 1977[15]; Melbourne et al. 1983[1]). "KAPRI" computes partial derivatives of the delay and delay-rate with respect to the obliquity of the mean ecliptic at J2000.0 as well as those with respect to the rate of general precession in longitude.

3.8 Time Epoch and Interval

The reference time system adopted in "KAPRI" is TDB which is the Solar system barycentric coordinate time. Since the VLBI observables are given in proper time, it is necessary to express delay and delay-rate in terms of TAI. On the other hand, it is necessary to compute TDB at a given epoch of TAI in evaluation of the astronomical arguments. Moyer (1981; see also the MERIT standards)[16] gave transformation formula between both time systems. "KAPRI" adopts the direct formula from ephemeris in computing TDB from TAI and the harmonic expansions in computing TDB from TAI. In the latter case, TDB is necessary to compute the astronomical arguments. However, difference between TAI and TDB other than a constant offset can be neglected in this case because the general relativistic corrections themselves are small. For the same reason, it is not necessary to convert the astronomical arguments in Moyer's expression from B1950 system to J2000.0 system.

3.9 Lorenzian Space Contraction

In the post Newtonian approximation, besides TAI-TDB difference, there is another relativistic effect which is large enough to affect the VLBI observables. It is space contraction by Lorenz effect (Fujimoto et al. 1982)[17]. It is given by:

$$\mathbf{R} = \mathbf{r} + (\beta - 1)\, \mathbf{v}\, \mathbf{v}^{\mathrm{T}} \cdot \mathbf{r} / \mathbf{v}^{\mathrm{T}} \cdot \mathbf{v}, \qquad \ldots\ldots (1)$$

where **R** and **r** are baseline vectors expressed by the solar system barycentric and geocentric coordinate system respectively, **v** is a velocity vector of the Earth around the Sun, and $\beta = (1 - v^2/c^2)^{-1/2}$.

3.10 Gravitational Bending of Radio Wave

The formula for the gravitational deflection of radio wave path due to the Sun includes the relativity index. The index is unity for Einstein's general relativity and 7/8 for Brans-Dicke's scalar-tensor theory. "KAPRI" has a capability of taking account of scalar-tensor theories. However, Einstein's relativistic formula (Shapiro 1967[18]; Murray 1983[19]) is usually adopted.

3.11 Coronal Delay

The effect of the solar corona is treated as bending of radio path. This effect is not usually important because radio sources near the Sun within about 10 degrees in the sky are not observed generally.

3.12 Ionospheric Delay

By observing at two frequencies it is possible to eliminate the main term of the ionospheric delay, which is the second order ($\propto 1/f^2$) in reciprocal of frequency (f). The elimination is made not in "KAPRI" but in another program (IONCR).

3.13 Atmospheric Delay

We adopt two models to express atmospheric delay and delay-rate. One is a simple modified cosecant law for the dry component of the atmosphere (Chao 1970[20]; Moran 1981[21]). The other is Marini's model which includes both the dry and wet components (Marini 1974)[22]. It is given by;

$$P = \bar{g}^{-1}\, (A+B)\, [\sin(\mathrm{el}) + B/(A+B) \times (\sin(\mathrm{el}) + 0.015)^{-1}] \qquad \ldots\ldots (2)$$

with

$$A = 0.002277\, [P_s + (1255/T_s + 0.05)\, e_s]$$

$$B = 0.002644 \exp(-0.00014372 \times H)$$

$$\bar{g} = 9.784\, (1 - 0.0026 \cos(2L) - 3.1 \times 10^{-7} H)$$

$$e_s = 6.11 \times 10^{[7.5 \times \{T_s - 273.16\} / \{237.3 + (T_s - 273.16)\}]},$$

where e_s is the pressure of water vapor at the ground, L and H are latitude and height of the observation site, T_s is atmospheric temperature and el is elevation. "KAPRI" has an option

to select either of them.

Another possibility of eliminating delay due to the wet component of the atmosphere is to use a water vapor radiometer (WVR) (Wu 1979)[23]. Kashima Station is equipped with a WVR; yet, it is not used in the present analysis.

4. Baseline Analysis

4.1 A priori Values of Station Positions and Star Catalog

We have used the Mark-III star catalog (#BLOKQ)[24] prepared by Chopo Ma and NGS star catalog. These catalogs come from the solution in which the data from 79AUG03 to 82JUN07 including POLARIS and NASA's surveys are used. In #BLOKQ, solution station positions are also adjusted, and clocks, atmospheres, and Polar-Motion and UT1 are adjusted for each day.

Table 2 A priori station positions.
Reference VLBI station is Mojave. Kashima position is transformed from Bessellian coordinate system. All positions are expressed by the VLBI coordinate system.

STATION		MOJAVE	KASHIMA	HATCREEK
POSITION (m)	X	-2356169.15	-3997894.93	-2523968.05
	Y	-4646756.83	3276580.09	-4123507.27
	Z	3668471.22	3724115.46	4147753.18
ANTENNA DIAMETER		12.2 m	26 m	26 m
BASELINE LENGTH (m)		MOJAVE – KASHIMA	8091824.75	
		MOJAVE – HATCREEK	729148.66	
		KASHIMA – HATCREEK	7557328.61	

Table 2 shows a priori values of three station positions. The positions of Mojave and Hat Creek are given by Chopo Ma of NASA/GSFC. Since the position of Mjoave is already adjusted by many other VLBI experiments, we tried to adjust the positions of Haystack and Kashima.

A priori position of Kashima given in the Bessellian coordinate system is transformed into the WGS72 (World Geodetic System 1972)[25] coordinate system, and then transformed from it into the VLBI coordinate system. The transformation from Bessellian coordinate (x, y, z) into WGS72 coordinate (X', Y', Z') is the shift of coordinate's origin such as $\Delta X = -140$ m, $\Delta Y = 516$ m, $\Delta Z = 673$ m. This transformation is shown in Eq. (3)[25]:

$$\begin{bmatrix} X' \\ Y' \\ Z' \end{bmatrix} = \begin{bmatrix} x + (-140) \\ y + 516 \\ z + 673 \end{bmatrix} \quad \text{(m)} \qquad \ldots\ldots\ldots\ldots\ldots\ldots\ldots\ldots\ldots\ldots (3)$$

The second transformation from WGS72 into VLBI coordinate (X, Y, Z) consists of the shift of coordinate's origin ($\Delta Z = 4$ m), a rotation about Z axis (+0.54 arcsec) and scale

multiplication $(1 + 0.3263 \times 10^{-6})$. This transformation is shown in Eq. (4):

$$\begin{bmatrix} X \\ Y \\ Z \end{bmatrix} = (1 + 0.3263 \times 10^{-6})\, Rz(-\theta) \begin{bmatrix} X' \\ Y' \\ Z' + 4 \end{bmatrix} \quad \text{(m)} \qquad \ldots\ldots\ldots\ldots\ldots\ldots (4)$$

where $Rz(-\theta)$ is a rotation matrix about Z axis ($\theta = +0.54$ arcsec).

We make baseline adjustment in the VLBI coordinate system.

4.2 Method of Baseline Adjustment

Two kinds of data are necessary for baseline adjustment. One stands for the observed delays and delay-rates (O). The other stands for the theoretical a priori delays and delay-rates (C), which include the contribution of ionospheric excess path.

(1) Least Squares Fits

Our basic approach for adjusting the parameters of interest is to use the linear least square adjustment for O−C residuals of delays and delay-rates.

We solve the following observation equation (Eq. (5)) which is weighted with observation errors based on the quality of the original observations.

$$WAX = WB \qquad \ldots\ldots\ldots\ldots\ldots\ldots\ldots\ldots\ldots\ldots\ldots\ldots\ldots\ldots\ldots\ldots\ldots\ldots (5)$$

$$A = \begin{bmatrix} \frac{\partial \tau_1(c)}{\partial a_1} & \frac{\partial \tau_1(c)}{\partial a_2} & \cdots\cdots \\ \frac{\partial \dot{\tau}_1(c)}{\partial a_1} & \frac{\partial \dot{\tau}_1(c)}{\partial a_2} & \cdots\cdots \\ \frac{\partial \tau_2(c)}{\partial a_1} & \frac{\partial \tau_2(c)}{\partial a_2} & \cdots\cdots \\ \cdots\cdots & \cdots\cdots & \end{bmatrix}$$

matrix of partial derivatives for delays and delay-rates

Here we define the weighted root mean square (r.m.s.) of delay and delay-rate. Eq. (6) shows the weighted r.m.s. of delay as well as that of delay-rate:

$$X = \begin{bmatrix} \Delta a_1 \\ \Delta a_2 \\ \vdots \end{bmatrix}$$

vector of adjustment parameters corrections such as baseline components, clock polynomials etc.

$$W = \begin{bmatrix} \frac{1}{\sigma_1^{\,2}(\tau_1)} & \cdots\cdots \\ \frac{1}{\sigma_1^{\,2}(\dot{\tau}_1)} & \cdots\cdots \\ \vdots & \cdots\cdots \end{bmatrix}$$

weighting matrix
$\sigma_i \propto (S/N)_i$
(S/N): signal to noise ratio.

$$B = \begin{bmatrix} \tau_1\,(O) - \tau_1\,(C) \\ \dot{\tau}_1\,(O) - \dot{\tau}_1\,(C) \\ \vdots \\ \vdots \\ \vdots \\ \vdots \\ \vdots \end{bmatrix}$$

vector of O–C residuals for delays and delay-rates.

$\tau_i\,(O), \dot{\tau}_i\,(O)$: observed delay and delay-rate for each occurrence (i) (an occurrence means one observation per baseline)

$\tau_i\,(C), \dot{\tau}_i\,(C)$: a priori delay and delay-rate for each occurrence (i) including the correction of the adjustment parameters

$$\text{weighted r.m.s.} = \sum_{i=1}^{N} \frac{(\tau_i\,(O) - \tau_i\,(C))^2}{\sigma_i^2\,(\tau_i)} \Bigg/ \sum_{i=1}^{N} \frac{1}{\sigma_i^2\,(\tau_i)} \quad \cdots\cdots\cdots\cdots\cdots\cdots (6)$$

N: number of observations, i: observation number.

(2) Re-weighting

There may be systematic errors after the weighted least square adjustment. So the statistical dispersion (Chi square χ^2) is larger than 1. We may add the constant formal errors (σ_{add} (delay), σ_{add} (rate)) to each observation error (σ_i, i = obs number), then the statistical dispersion becomes approximately equal to 1 for each baseline. We call this process "re-weighting".

Eq. (7) and Eq. (8) show the methods of computing the added formal error and re-weighting respectively for each baseline.

$$\chi^2\,(\text{delay}) = \frac{1}{N - N_P} \sum_{i=1}^{N} \left\{ \frac{(\tau_i\,(O) - \tau_i\,(C))^2}{\sigma_i^2\,(\tau_i) + \sigma_{add}^2(\text{delay})} \right\} = 1$$

$$\chi^2\,(\text{rate}) = \frac{1}{N - N_P} \sum_{i=1}^{N} \left\{ \frac{(\dot{\tau}_i\,(O) - \dot{\tau}_i\,(C))^2}{\sigma_i^2\,(\dot{\tau}_i) + \sigma_{add}^2(\text{rate})} \right\} = 1 \quad , \quad \cdots\cdots\cdots\cdots\cdots\cdots (7)$$

σ_{add}(delay), σ_{add}(rate): the constant added formal errors of delay and delay-rate respectively for each baseline.

$$W_{add}\,A\,X = W_{add}\,B$$

$$W_{add} = \begin{bmatrix} \frac{1}{\sigma_1^2\,(\tau_1) + \sigma_{add}^2(\text{delay})} & \cdots \\ & \\ \frac{1}{\sigma_1^2\,(\dot{\tau}_1) + \sigma_{add}^2(\text{rate})} & \cdots \end{bmatrix} \quad \cdots\cdots\cdots\cdots\cdots\cdots\cdots\cdots (8)$$

Our final results of baseline adjustment are those of the re-weighted least square adjustment. The weighted r.m.s. of re-weighting is expressed by an equation which is almost the same as Eq. (6).

(3) Ambiguity

There are some ambiguities of observed delays which are multiplicative of 100 ns in X-band and of 200 ns in S-band. All data are corrected by the "suitable ambiguities" of observed delays.

(4) Exclusion of Bad data

There are some observations which are not used for adjusting some parameters, called "bad data". We adopt the following three definitions of "bad data":

1. quality code of bandwidth synthesis is 0
2. closure observed delay greater than 0.2 nsec or closure observed delay-rate greater than 0.2 psec/sec in X-band
3. ionospheric correction in X-band is wrong, that is, closure delay of a priori values corrected for ionosphere is greater than 0.2 nsec.

In the above definition, the quality code of bandwidth synthesis shows the condition of bandwidth synthesis; code 0 shows worst data, and code 10 means completely good data in band width synthesis.

There are 50 bad data derived from our results of data processing and 25 bad ones derived from Mark-III processing.

(5) Selection of Adjusted Parameters

We should select some parameters to be adjusted, such as zenith excess path of atmosphere, clock polynomials, baseline components, Earth orientation parameters and source positions.

1) Clock Polynomials

We set the epochs and the numbers of terms of clock polynomials in order to minimize O–C residuals. The number of terms is generally two, corresponding to clock offset and clock-rate. The epoch of clock polynomials is a time when the behavior of O–C residuals of all stars jumps or bends together. It depends on an operator's judgment. Fig. 3 shows the clock epochs and the behavior in the present experiments which is mainly caused by clock offset and clock-rate.

2) Atmosphere and Source Position

Even if some clock polynomials are adjusted, the residual pattern for some sources shows some systematic behavior which is different from that of other sources. Part of the trend may be caused by the inaccurate theoretical values of the atmospheric effect at low elevation angles. As the elevation decreases, the residuals for a source show a systematic departure from the behavior of the other sources, leading generally to larger residuals. In this case we set the additional epochs for atmospheric models and adjust the zenith excess-paths at the additional epochs.

When its systematic departure for some source remains after the adjustments for the zenith excess-paths, we adjust the source positions.

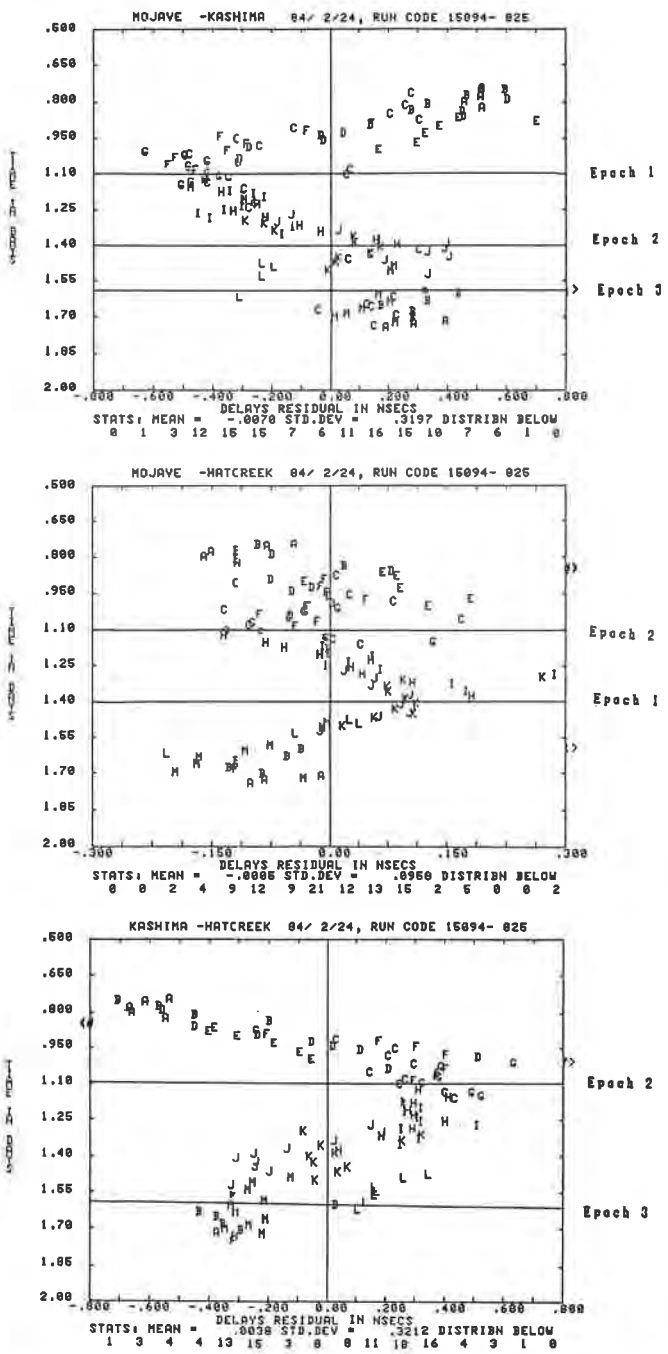

Fig. 3 Clock Epoch of Clock offset and Clock rate.
The abscissa is O-C residual (nsec) and the ordinate is observation time from the start of experiments. Each alphabet shows each star in this figure.

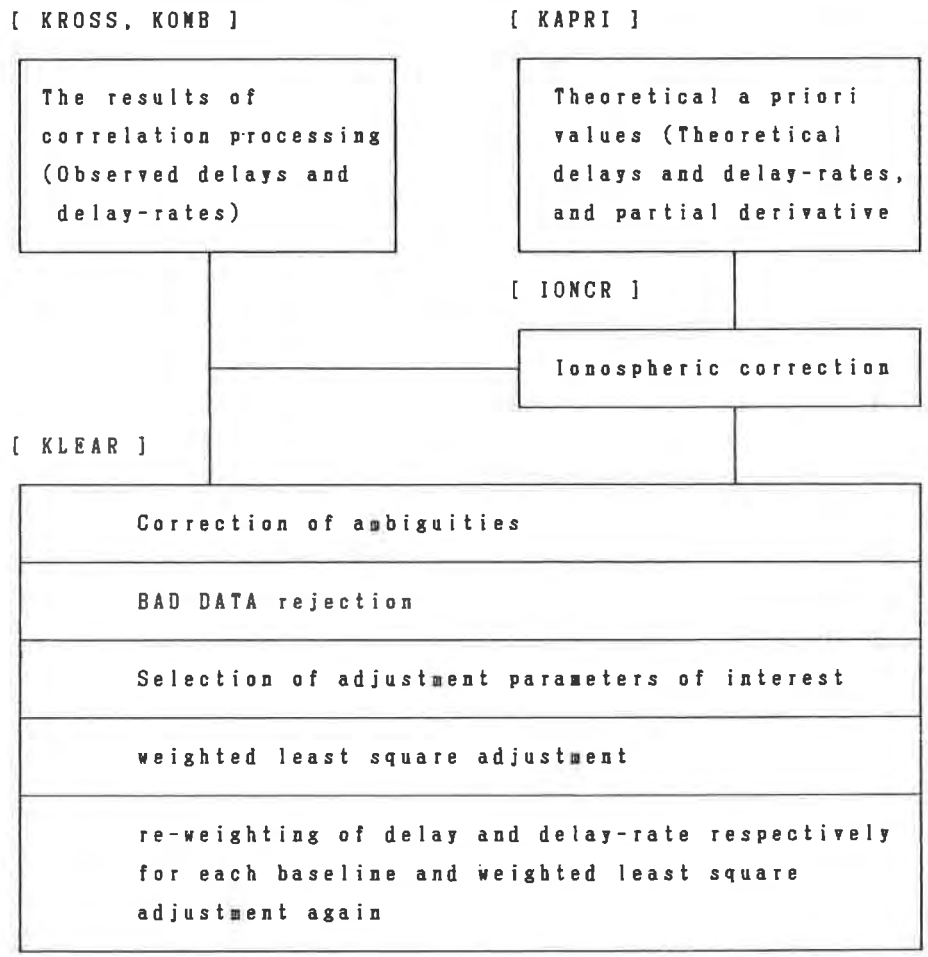

Fig. 4 Flow of the baseline adjustment.

Fig. 4 shows the process of the baseline adjustment. First, we correct the suitable ambiguities, secondly we exclude the bad data. Then we set the clock polynomials and atmospheric parameters for each station, and baseline components for each baseline. We adjust these parameters by solving the weighted observation equation (Eq. 5). Lastly we re-weight for above solutions. Fig. 5 shows O–C delay residuals of our final results in the February experiment, in which Marini model, BIH data, Yoder's UT1 Earth tide correction model and #BLOKQ star catalog without the adjustment of star position are used.

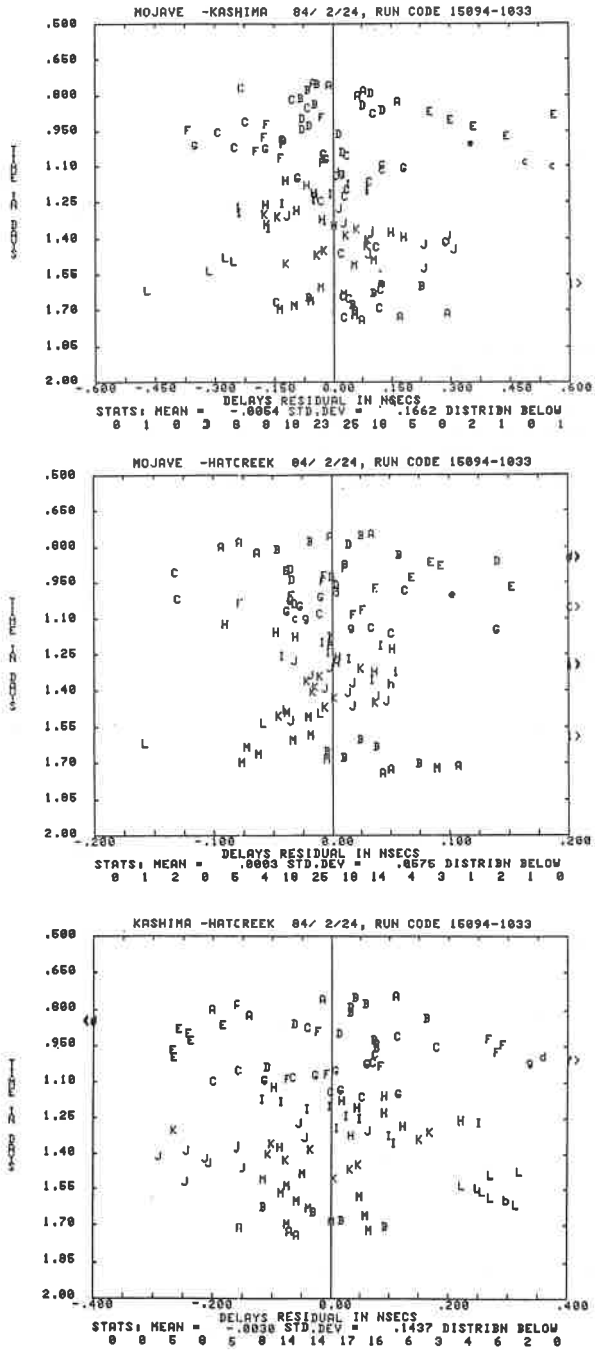

Fig. 5 The O-C residual pattern of the final results in February Experiment. The abscissa and the ordinate are the same as Fig. 3.

4.3 Result of Baseline Analysis

We adjust some parameters of interest by using delays and delay-rates, with one baseline in the January experiment and three baselines in the February experiment.

(1) Comparison between Kashima Processing Data and Haystack Processing Data

There are 301 occurrences for the analysis of Kashima processing data, and 330 occurrences for Haystack processing data. The difference of the number is caused by the number of bad data. Almost the same analysis results are obtained by both data (See Table 3). The small differences between both analysis results are mainly caused by the difference of the number of used data.

Table 3 The results of the system-level experiments for GSFC and Kashima analyses and repeatability of the January and February experiments. The results are obtained by using BIH earth rotation parameters, Mark-III star catalog and Marini atmospheric model. We use both delays and delay-rates, with 3 baselines in the February experiment, and with 1 baseline in the January experiment. ( ) are adjustment errors.

	ADJUSTMENT OF KASHIMA POSITION X (m)	Y (m)	Z (m)	BASE LINE LENGTH OF KASHIMA-MOJAVE (m)	WEIGHTED RMS DELAY (ns)	RATE (ps/s)
JANUARY EXPERIMENT						
HAYSTACK PROCESSING AND GSFC ANALYSIS	3.88 (0.04)	0.13 (0.04)	3.62 (0.04)	8091824.11 (0.04)	0.180	0.143
HAYSTACK PROCESSING AND KASHIMA ANALYSIS	3.70 (0.03)	0.09 (0.03)	3.50 (0.03)	8091824.11 (0.03)	0.198	0.063
FEBRUARY EXPERIMENT						
HAYSTACK PROCESSING AND GSFC ANALYSIS	4.60	0.26	3.59	8091824.09	–	–
HAYSTACK PROCESSING AND KASHIMA ANALYSIS	4.62 (0.03)	0.29 (0.02)	3.64 (0.03)	8091824.13 (0.02)	0.091	0.055
KASHIMA PROCESSING AND KASHIMA ANALYSIS	4.55 (0.03)	0.25 (0.03)	3.75 (0.03)	8091824.09 (0.03)	0.110	0.083

(2) Baseline Analyses in Kashima and GSFC

The staff of both Kashima and Goddard Space Flight Center (GSFC) make baseline analyses by using BIH data and Marini atmospheric model, and almost the same other physical models. The position of Kashima Station is decided by us within a few-centimeter differences from GSFC's ones, in the February experiment (See Table 3).

Baseline length between Mojave and Kashima is determined with a difference of a few mm between the results of two analyses in the January experiment, and with the differences of several centimeters in the February experiment.

These differences come from the model difference adopted for the UT1 correction by

Earth tide, and the adjustment parameters of interest.

(3) Repeatability

Since we carry out two system-level experiments, we can compare two results of the January and February experiments. In the results of two experiments, BIH data, Marini atmospheric model and other physical models are used.

The baseline difference between two experiments is about 0.9 m in X component, about 0.2 m in Y component, about 0.1 m in Z component, and 0.02 m in baseline length (See Table 3).

Since this 3-baseline configuration is an extremely flat triangle, we cannot adjust the Earth orientation parameters, such as UT1 and Wobble. This means that we cannot exactly decide X, Y, Z components since they couple to the Earth orientation parameters. However, the Earth orientation parameters do not have any systematic effects on baseline-length because the Earth rotation parameters have relation only to the baseline direction. That is why we can decide it in good repeatability, in such a way that the baseline length between Kashima and Mojave is 801924.13 m in February and 801924.11 m in January.

(4) Earth Orientation Parameters

We do not try to adjust the Earth orientation parameters, but we use IPMS or BIH data as unadjusted parameters. We compare the results of IPMS data with those of BIH data by using Marini atmospheric model in the February experiment.

The differences in adjustments between IPMS and BIH data are 0.024 arcsec in wobble X component, −0.005 arcsec in wobble Y component, −0.005 timesec in UT1 in the February experiment.

By these differences, the analysis results obtained by using IPMS data are smaller by 0.26 m in X component, by 0.05 m in Y component, by 0.39 m in Z component than those

Table 4 Comparison of IPMS data with BIH data
The results are obtained by using MARINI atmospheric model and Mark-III star catalog. In the UT1 correction of earth tide, YODER model is adopted. The delays and delay-rates are used together, with 3 baselines in the February experiment and with 1 baselines in the January experiment.

	IPMS	BIH
KASHIMA POSITION ADJUSTMENT		
X (m)	4.36 ± 0.02	4.62 ± 0.03
Y (m)	0.24 ± 0.02	0.29 ± 0.02
Z (m)	4.03 ± 0.03	3.64 ± 0.03
KASHIMA-MOJAVE BASELINE LENGTH (m)	8091824.13 ±0.02	8091824.13 ±0.02
WEIGHTED RMS OF 3 BASELINES		
DELAY (nsec)	0.090	0.091
RATE (ps/s)	0.057	0.057
WEIGHTED RMS OF KASHIMA-MOJAVE		
DELAY (nsec)	0.162	0.165
RATE (ps/s)	0.072	0.071

obtained by using BIH data. However, we cannot decide which data is better. The baseline length is the same because the difference between IPMS and BIH data is just caused by the rotation on transformation and does not affect the baseline length (See Table 4).

(5) Atmospheric Model

We adopt two atmospheric models, one is Marini model, the other is Chao/Moran model, both of which are usually used by NASA/GSFC group. Marini model includes a water vapor excess path; on the other hand, Chao/Moran model includes only an excess path in a dry atmosphere. Both models are not perfect, so we should adjust the atmospheric effect. Its adjusted parameter is a zenith excess path. We adjusted it by using the partial derivative of Chao model with regard to elevation angle. The results of baseline analysis by using Marini model are smaller by 0.02 m in X component, by −0.03 m in Y component and by −0.01 m in Z component, and by 0.03 m in baseline length than those by using Chao/Moran. The weighted r.m.s. of the residuals by using Marini model is smaller than that by Chao/Moran Since the difference is small, we cannot determine which model is better (See Table 5).

Table 5 Comparison of Marini model or Moran/Chao atmospheric model. The results are obtained by using BIH earth rotation parameters and Mark-III star catalog. In The UT1 correction of earth tide, YODER model is adopted. The delays and delay-rates are used together, with 3 baselines in the February experiment, with 1 baselines in the January experiment.

	MARINI	CHAO/MORAN
KASHIMA POSITION ADJUSTMENT		
X (m)	4.62 ± 0.03	4.64 ± 0.02
Y (m)	0.29 ± 0.02	0.26 ± 0.02
Z (m)	3.64 ± 0.03	3.63 ± 0.03
KASHIMA-MOJAVE BASELINE LENGTH (m)	8091824.13 ±0.02	8091824.09 ±0.02
WEIGHTED RMS OF 3 BASELINES		
DELAY (nsec)	0.091	0.094
RATE (ps/s)	0.057	0.055
WEIGHTED RMS OF KASHIMA-MOJAVE		
DELAY (nsec)	0.165	0.154
RATE (ps/s)	0.071	0.070

5. Remarks on Star Catalog

We have used the Mark-III star catalog of #BLOKQ.[24] The residual pattern for 3C273B shows a systematic behavior which is different from those of other sources on a long baseline. Its systematic behavior is caused by three effects: atmosphere-effects, clock-effects and star positions configurations. When we adjust the right ascension of 3C273B, we find the systematic shift of about −3 milliarcsec in case we use the #BLOKQ's one.

We use another star catalog (JPL 1983-5) made by JPL group. The right ascension of 3C273B is the reference of the other sources. For the 3C273B, both right ascensions of #BLOKQ and JPL catalogs are the same, i.e. 12h42m6.6997s. The average of the differences

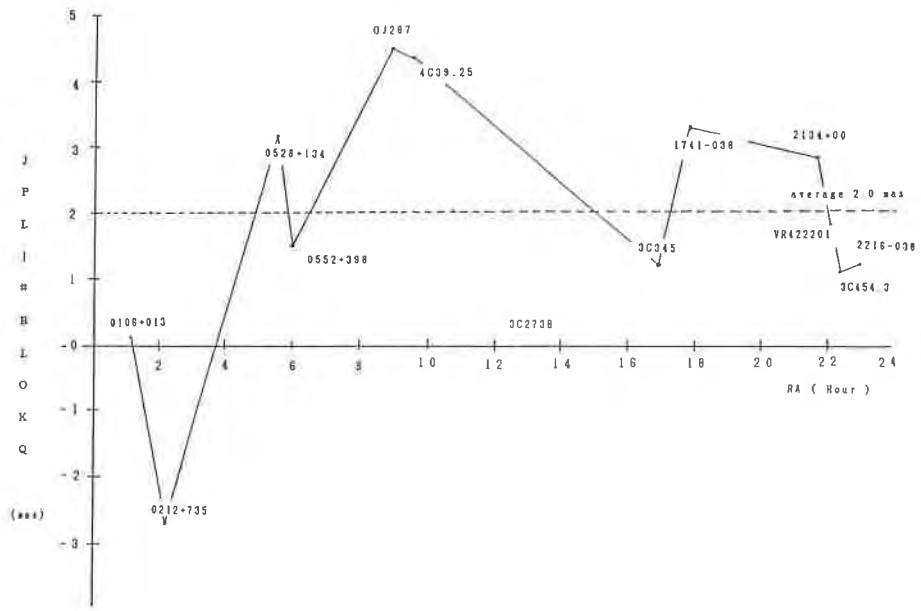

Fig. 6 The differences of the right ascensions between JPL star catalog and #BLOKQ (reference) in the system-level experiments. The ordinate is JPL−#BLOKQ of the right ascension in marcsec unit and the abscissa is the right ascension of the star in hour unit.

between #BLOKQ and the JPL star catalog is about 2 milliarcsec in right ascension, as shown in Fig. 6. We compare the adjustments of the right ascensions observed in the present experiments by using two star catalogs. The behavior of adjustments has the same systematic behavior as shown in Fig. 6.

The differences of the baseline components and that of baseline-length determined by these two star catalogs are only a few centimeters. On the other hand, the difference in the systematic error is larger than them. The systematic error by using the JPL star catalog is smaller than that by using #BLOKQ. Moreover, our adjustment of 3C273B's right ascension is almost the same as the average of the differences between two star catalogs in the present experiments. So the JPL star catalog is more consistent with the present experiments.

If, however, we want to know exactly the positions of the stars, we should accumulate VLBI data because the systematic error may be caused by other reasons such as the atmospheric model and clock polynomials.

6. Discussion

6.1 Systematic Error

The observation errors of delay and delay-rate, $\sigma(\tau)$ and $\sigma(\dot{\tau})$, are produced by "KOMB" respectively. They are related to observation parameters such as the sensitivity of telescopes, the intensity of radio sources and an arrangement of frequency channels in a receiving system. These errors in the present experiments are approximately evaluated as:[27]

$$\sigma(\tau) = 0.40 \,/\, \mathrm{SNR\ (nsec)}$$
$$\sigma(\dot{\tau}) = 0.073 \,/\, \mathrm{SNR\ (psec/sec)}. \qquad \cdots\cdots (9)$$

where the SNR, Signal-to-Noise Ratio, shows the quality of correlated data in a receiving channel. The SNR varies with the observed star and the baseline. Since the SNR of 4 ~ 40 is obtained in the present experiments, the observation errors of delay are estimated to be 0.01 ~ 0.1 nsec (typical value 0.04 nsec) and the observation errors of delay-rate are estimated to be 0.002 ~ 0.02 psec/sec (typical value 0.008 psec/sec).

On the other hand, the closure delay and delay-rate have an r.m.s. of 0.08 nsec and 0.02 psec/sec, respectively. These values are in a range of estimated errors of delay and delay-rate, when we consider the fact that the closure value is a linear combination of three observations and the error of the closure value is obtained by multiplying the error of one baseline by $\sqrt{3}$. So delay and delay-rate observed in the present experiments are reasonable enough to make baseline analyses and to determine baseline components precisely.

On the contrary, the errors of 0.10 nsec and 0.06 psec/sec remain in delay and delay-rate after the final adjustment. These errors are two or three times as large as the observation errors. This discrepancy between them tells us the existence of the systematic error omitted in the present analyses.

We compare the residual errors on each baseline. After re-weighted least square adjustment, there is still a small systematic error of delay. Its maximum value is smaller than 0.6 nsec and its r.m.s. value is about 0.17 nsec. The residual errors of delay-rate at the three baselines are almost the same (0.04 ~ 0.07 psec/sec) with one another. However, the residual errors of delay vary with the baseline. In fact, they are large in the case of long baselines. The contributions of the source structure, atmospheric effects and clock offset to delay are large, but not to delay-rate except the observation with the low elevation angle.

The systematic error is mainly caused by the imperfect adjustment of atmospheric effects and clock offsets. Also the systematic error is caused by the uncertainty of star positions and source structures.

6.2 Source Structure Contribution

The contributions of source structure are smaller than 0.1 nsec in delays and 0.01 psec/sec in delay-rates in the present experiments. These contributions to delays are of almost the same order as the weighted r.m.s. of delays. So they do not have any large effects on the baseline adjustment, but they have certain effects on the weighted r.m.s. of delays.

6.3 Earth Orientation Parameters

If we can include the Earth orientation parameters (EOP) in our analysis, we can determine the position of Kashima 3-dimensionally, such as X, Y, Z. So we examine the possibility of making the adjustment for the EOP in the following two cases.

One baseline experiment

Even if the positions of two stations are exactly known, all parameters of the EOP cannot be adjusted, but only two of them can be adjusted. If the positions are not known, we can do nothing for the EOP but estimate the positions.

Three baseline-experiment

If the positions of three stations are known, the EOP can be adjusted completely. If the positions of two stations are known, two EOP can be adjusted together with the third position of station.

In the case of our present experiments, we obtain data on three baselines; however we cannot adjust the EOP because the baselines from Kashima to the U.S. stations are in almost East-West direction and low independency. Therefore, we needed data about the EOP to deduce 3-dimensionally the position of Kashima.

First, we use BIH or IPMS data in the present experiments, and obtain results shown in Table 3. In the table, we can see the considerable discrepancy between the results in the present two experiments.

Next, we use IRIS data and get good agreement between them, because the IRIS data come from a large amount of VLBI observations and they are consistent with our VLBI experiments. The result by using IRIS data will be referred in the future publication.

7. Conclusion

As mentioned above, the Japan-U.S. joint VLBI system-level experiments showed that K-3 system has satisfactory performance and good compatibility with Mark-III.

We attained the following five results of the baseline adjustment.

1) Correlation processing of K-3 system was made correctly except the large variance of delay-rate closure. This means that the baseline analysis using these data on K-3 system was reasonable.
2) The baseline length between Kashima and Mojave is 8091824.11 m and its precision is 0.02 m. Its accuracy is unknown, but we will be provided with the accuracy gradually by many global VLBI experiments such as multi-baseline West Pacific experiment (WPAC).
3) The components of position of Kashima Station in the VLBI coordinate system are adjusted as −3997890.31 m in X, 3276580.38 m in Y, 3724119.10 m in Z, respectively, and the precision of each of X, Y, and Z is around 0.03 m for the February experiment. The Earth orientation parameters issued by BIH data and Marini atmospheric model are used for the February experiment. However, we cannot determine the Earth rotation parameters for the reason that the baselines from Kashima to the U.S. stations are in almost East-West direction. The result of analysis with IPMS data is smaller than the result with BIH data by about 0.26 m in X, by 0.05 m in Y and by −0.39 m in Z in the February experiment.
4) A priori values of the components of Kashima position are given from the Bessellian coordinate system. They are transformed into the VLBI coordinate system to be used together with the other U.S. stations in the VLBI coordinate system. The differences between a priori values and the VLBI results in the present experiments are 4.6 m, 0.3 m and 3.6 m in X, Y and Z respectively at the Kashima Station. These differences show that a transformation from the Bessellian coordinate into the VLBI coordinate may not be suitably corrected.
5) The residuals of the reference star, 3C273B, are systematically larger than those of the other star. Its behavior shows the departure from those of the other star. A part of the systematic trend of 3C273B is caused by Mark-III star positions.

We participated in Crustal Dynamics Project in the summer of 1984 (WPAC and POLAR experiments of NASA). We carried out two West Pacific experiments (WPAC) on 28-30 July and 4-6 August 1984. Five stations, such as Kashima, Mojave (California), Kauai (Hawaii), Kwajalein (Marshall Islands), Fairbanks (Alaska), participated in these experiments. Each experiment was conducted for 2 days and the number of total occurrences was about 4000. The baseline analyses of WPAC and POLAR will show many new results, e.g. the position of Kashima.

Acknowledgment

We wish to thank Drs. N. Kawano, F. Takahashi and Mr. N. Kawaguchi as well as other members of the VLBI group in Radio Research Laboratory (RRL). We also wish to express our thanks to Messrs. T. Sato and H. Hanada of International Latitude Observatory of Mizusawa (ILOM) for computing the ocean tidal effects on site displacement at Kashima and other VLBI stations. We would like to thank Mr. T. Ishikawa and Dr. M. Fujishita of ILOM for converting part of "KAPRI" developed at the ILOM to work on HP1000 at Kashima.

References

(1) Melbourne, W., Anderle, R., Feissel, M., King, R., McCarthy, D., Smith, D., Tapley, B. and Vicente, R.; "MERIT STANDARD", United States Naval Observatory Circular, 167, 1983.

(2) Cartwright, D.E. and Tayler, R.J.; "New computations of the tide-generating Potential", Geophys. J.R. Astron. Soc., **23**, 45, 1971.

(3) Cartwright, D.E. and Edden, A.C.; "Corrected Tables of Tidal Harmonics", Geophys. J.R. Astron. Soc., **33**, 253, 1973.

(4) Wahr J.M.; "Body tides on an elliptical, rotating, elastic and oceanless earth", Geophys. J.R. Astron. Soc. **64**, 677, 1981.

(5) Schwiderski, E.W.; "Grobal ocean tide, part I: a detail hydrodynamical interpolation model", Rep. TR-3866, U.S. Naval Surface Weapons Center, 1978.

(6) Farrell, W.E.; "Deformation of the earth by surface loads", Rev. Geophys. Space Phys., **10**, 761, 1972.

(7) Sato, T. and Hanada, H.; "A program for the computation of oceanic tidal loading effects 'GOTIC' ", Publ. Int. Latit. Obs. Mizusawa, **18**, 29, 1984.

(8) Goad, C.; "Gravimetric tidal loading computed from integrated Green's function", J. Geophys. Res., 85, 2679, 1980.

(9) Alaterman, Z., Jarosch, H. and Pekeris, C.L.; "Propagation of Rayleigh wave in the earth", Geophys. J.R. Astron. Soc., **4**, 219, 1961.

(10) Yoder C.F., Williams J.G., Parke M.E.; "Tidal variations of earth rotation", J. Geophys., **86**, B2, 881, 1981.

(11) Naito, I. and Yokoyama, K.; a report presented at Sopron, Hungary, 1984.

(12) Wahr, J.M.; "The forced nutations of an elliptical, rotating, elastic and oceanless earth", Geophys. J.R. Astron. Soc., **64**, 705, 1981.

(13) Kinoshita, H.; "Theory of the rotation of the rigid earth", Cel. Mech., **15**, 277, 1977.

(14) Gilbert, F. and Dziewonski, A.M.; "An application of normal mode theory to the retrieval of structural parameters and source mechanics from seismic spectra", Phil. Trans. R. Soc. London, A278, 187–269, 1975.

(15) Lieske J.H.; "Expression for the Precession quantities based upon the IAU (1976) System of Astronomical Constants", Astron. Astrophys, **58**, 1977.
(16) Moyer T.D.; "Transformation from proper time on earth to coordinate time in solar system barycentric space-time frame of reference", Cel. Mech., **23**, part 1, 2, 33–68, 1981.
(17) Fujimoto, M.K., Aoki, S., Nakajima, K., Fukushima, T. and Matsuzaka, S.; "General relativistic framework for the study of Astronomical/Geodetic reference coordinate", NOAA Tech. Rep. NOS 95 NGS 24, 26, 1982.
(18) Shapiro; "New method for the detection of light deflection by solar gravity", Science, **157**, 806, 1967.
(19) Murray, C., A.; "Vectorial Astrometry", Chap. 2, Adam Hilger, Bristol, Great Britain, 1983.
(20) Chao, C.C.; "A preliminary estimation of Tropospheric influence on the range and range rate data during the closest approach of the MM71 Mars Mission", JPL Tech. Memo, 391, 1970.
(21) Moran J.M., Rosen B.R.; "Estimation of the propagation delay through the troposphere from microwave radiometer data", Radio Science, **16**, 2, 235, 1981.
(22) Marini, J.W.; private communication, 1984.
(23) Wu, S.C.; "Optimum frequencies of a passive microwave radiometer for tropospheric path length correction", IEEE Transaction on Antennas and Propagation, AP-27, 2, 1979.
(24) Chopo Ma; "#BLOKQ", private communication, 1984.
(25) Seppelin, T., O.; "The Department of Defense World Geodetic System 1972", The Canadian Surveyor, **28**, 5, 1974.
(26) Hothem, L., D.; "Determination of accuracy, orientation and scale of satellite doppler point-positioning coordinates" Proc. Second Intern. Geodetic Symp. on Satellite Doppler Positioning, Austin, 1979.
(27) Kawaguchi N.; "Coherence loss and delay observation error in Very-Long-Baseline Interferometry", J. Radio Res. Lab., **30**, 129, 59, 1983.